Title

Morphology–Conductivity Relationship of Single-Ion-Conducting Block Copolymer Electrolytes for Lithium Batteries

Journal

ACS Macro Letters, 3(6)

ISSN

2161-1653

Authors

Inceoglu, Sebnem
Rojas, Adriana A
Devaux, Didier
et al.

Publication Date

2014-06-17

DOI

10.1021/mz5001948

Peer reviewed

ACS Macro Letters

Letter

pubs.acs.org/macroletters

Morphology–Conductivity Relationship of Single-Ion-Conducting Block Copolymer Electrolytes for Lithium Batteries

Sebnem Inceoglu,[†,⊥] Adriana A. Rojas,[‡,§,⊥] Didier Devaux,[‡] X. Chelsea Chen,[†] Greg M. Stone,[∥] and Nitash P. Balsara*[,†,‡,§,⊥]

[†]Materials Sciences Division, Lawrence Berkeley National Laboratory, Berkeley, California 94720, United States

[‡]Environmental Energy Technologies Division, Lawrence Berkeley National Laboratory, Berkeley, California 94720, United States

[§]Department of Chemical and Biomolecular Engineering, University of California, Berkeley, California 94720, United States

[⊥]Joint Center for Energy Storage Research (JCESR), Lawrence Berkeley National Laboratory, Berkeley, California 94720, United States

[∥]Malvern Instruments Inc., 117 Flanders Road, Westborough, Massachusetts 01581, United States

Supporting Information

ABSTRACT: A significant limitation of rechargeable lithium-ion batteries arises because most of the ionic current is carried by the anion, the ion that does not participate in energy-producing reactions. Single-ion-conducting block copolymer electrolytes, wherein all of the current is carried by the lithium cations, have the potential to dramatically improve battery performance. The relationship between ionic conductivity and morphology of single-ion-conducting poly(ethylene oxide)-*b*-polystyrenesulfonyllithium(trifluoromethylsulfonyl)imide (PEO–PSLiTFSI) diblock copolymers was studied by small-angle X-ray scattering and ac impedance spectroscopy. At low temperatures, an ordered lamellar phase is obtained, and the "mobile" lithium ions are trapped in the form of ionic clusters in the glassy polystyrene-rich microphase. An increase in temperature results in a thermodynamic transition to a disordered phase. Above this transition temperature, the lithium ions are released from the clusters, and ionic conductivity increases by several orders of magnitude. This morphology–conductivity relationship is very different from all previously published data on published electrolytes. The ability to design electrolytes wherein most of the current is carried by the lithium ions, to sequester them in nonconducting domains and release them when necessary, has the potential to enable new strategies for controlling the charge–discharge characteristics of rechargeable lithium batteries.

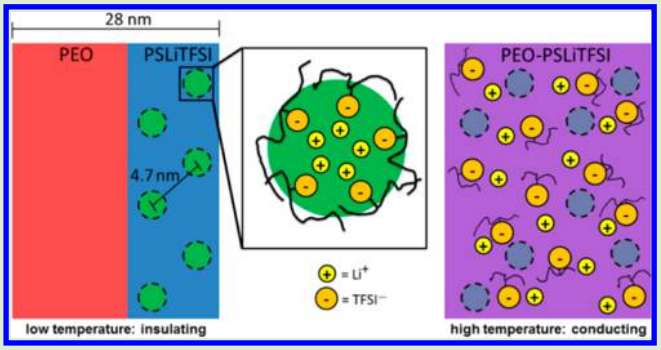

Single-ion-conducting polymer electrolytes, with ionic groups covalently bonded to the polymer and free counterions, are fundamentally different from conventional electrolytes wherein salts comprising positive and negative ions are dissolved in either liquid or polymeric solvents.[1−3] A popular example of a single-ion-conducting electrolyte is hydrated Nafion wherein negatively charged sulfonate groups are fixed onto a fluorinated polymer backbone while the associated hydronium counterions are mobile.[4,5] Transport of counterions in such systems occurs in the absence of concentration gradients provided that the bound ion concentration is uniform. This follows from the electroneutrality constraint. The performance of batteries and fuel cells with single-ion-conducting electrolytes is predicted to be superior to that obtained using conventional electrolytes, due to the absence of concentration polarization effects.[2] Commercial lithium-ion batteries contain electrolytes where a majority of the current is carried by the ion that does not participate in energy-producing reactions. It has long been recognized that dramatic improvements in batteries can be realized if single-ion conductors with high ionic conductivity can be designed.

In this paper, we focus on single-ion conductors containing "mobile" lithium ions. Most of the studies on such materials are limited to single-phase systems wherein ionic groups are covalently attached to homopolymers.[6,7] Dramatically different single-ion conductors based on block copolymers were first proposed by Ryu et al.[8] and more recently by Bouchet et al.[9] The work in ref 9 is based on polystyrene-*b*-poly(ethylene oxide)-*b*-polystyrene triblock copolymers, wherein lithium bis(trifluoromethane)sulfonamide (LiTFSI) was covalently linked to styrene units in the polystyrene blocks. Polystyrene (PS) and poly(ethylene oxide) (PEO) chains are highly incompatible.[10] Extensive works on the thermodynamics of polystyrene-*b*-poly(ethylene oxide) (SEO) copolymers with

Received: April 1, 2014
Accepted: May 12, 2014
Published: May 15, 2014

   dx.doi.org/10.1021/mz5001948 | *ACS Macro Lett.* 2014, 3, 510–514

added lithium salts, particularly LiTFSI, indicate that the tendency for microphase separation is enhanced by the presence of ions.[11,12] One thus expects microphase separation in the triblock copolymers, but no evidence for the presence or absence of such effects was reported in ref 9. The ionic conductivities of these single-ion-conducting triblock copolymers[9] were similar to that of mixtures of SEO and LiTFSI.[13] In contrast, the cation transference number of these triblock copolymers was in the vicinity of unity, well above typical values obtained in electrolytes containing lithium salts (between 0.1 and 0.5).[14−18]

In Figure 1, we show a schematic of lithium ion migration in a microphase-separated poly(ethylene oxide)-*b*-polystyrenesulfonyllithium(trifluoromethylsulfonyl)imide diblock copolymer (PEO−PSLiTFSI) electrolyte. The most interesting aspect of these electrolytes is that "mobile" lithium counterions are ionically bound to the immobile and glassy polystyrene blocks. Transport of lithium ions can only occur if they migrate from the PS-rich microphase into a PEO-rich environment. The expected scenario is illustrated in Figure 1. The main purpose of this study is to describe the effect of lithium ion migration on morphology in single-ion-conducting block copolymer electrolytes.

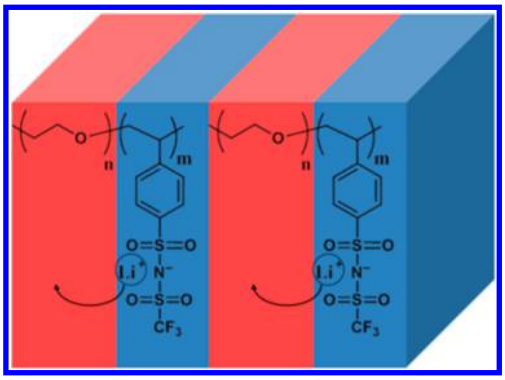

Figure 1. Schematic of lithium ion migration in a single-ion-conducting block copolymer electrolyte.

Poly(ethylene oxide)-*b*-polystyrenesulfonyllithium-(trifluoromethylsulfonyl)imide diblock copolymers (PEO−PSLiTFSI) were synthesized by following the previously reported procedures.[9,19] In this study, we focus on a particular copolymer, PEO−PSLiTFSI(5.0−3.2) where 5.0 and 3.2 are the molecular weights in kg mol^{-1} of the PEO and PSLiTFSI blocks. The ratio of lithium ions to ethylene oxide monomers, r, is 0.088. We also present results obtained from a PEO−PSLiTFSI(5.0−2.0) diblock copolymer with r = 0.056.

Small-angle X-ray scattering (SAXS) intensities, I, as a function of the magnitude of the scattering vector, q, of PEO−PSLiTFSI(5.0−3.2), obtained during a heating run, are shown in Figure 2a. At room temperature, the scattering profile indicates the presence of a lamellar morphology, with a primary scattering peak at $q = q^* = 0.228$ nm^{-1}, and higher-order scattering peaks in the vicinity of $2q^*$, $3q^*$, and $4q^*$. The location of the higher-order peak in the vicinity of $2q^*$ differs substantially from the calculated value. Observed SAXS peak locations may be affected by the low-q up-turn (Figure 2). Similar up-turns have been observed in other charged block copolymers.[20] The domain spacing, d, defined as the center-to-center distance between adjacent PEO-rich lamellae is 28 nm ($d = 2\pi/q^*$). SEO copolymers with comparable molecular weights exhibit d spacing in the vicinity of 15 nm.[21] While the addition of charges on the chain is expected to increase d spacing, the observed magnitude of this increase is surprising.

An additional SAXS peak is observed at $q = q_c = 1.33$ nm^{-1} (Figure 2a). Similar peaks have been observed in a wide variety of ionomers including polystyrenesulfonate, Nafion, and sulfonated polyesters.[4,5,22−24] We thus conclude that the TFSI$^-$ and Li$^+$ ions are clustered at room temperature in PEO−PSLiTFSI(5.0−3.2). The average distance between clusters, $d_{cluster}$, is approximately 4.7 nm ($d_{cluster} = 2\pi/q_c$). Heating the sample results in a decrease of peak intensities as shown in Figure 2a. Scattering peaks indicative of the lamellar structure are absent at temperatures above 50 °C. The intensity of the ion cluster peak also decreases substantially above 50 °C (Figure 2b). Changes in the scattering intensity are reversible. The lamellar peaks are obtained during the cooling run at temperatures below 45 °C as shown in Figure 2c. The intensity of the ion cluster peak also increases as the sample is cooled

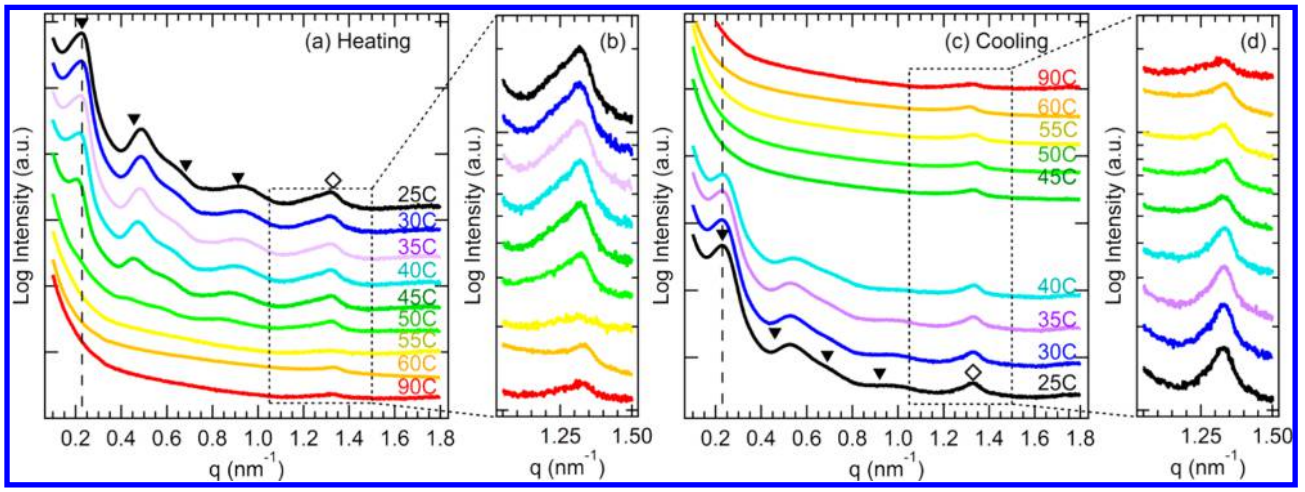

Figure 2. Temperature dependence of SAXS for the PEO−PSLiTFSI electrolyte. (a) SAXS intensity versus scattering vector, q, during a heating scan. (b) Scattering in the vicinity of the ion cluster peak during a heating scan. (c) SAXS intensity versus scattering vector, q, during a cooling scan. (d) Scattering in the vicinity of the ion cluster peak during the cooling scan of PEO−PSLiTFSI(5.0−3.2), r = 0.088.

dx.doi.org/10.1021/mz5001948 | *ACS Macro Lett.* 2014, 3, 510−514

(Figure 2d and Figure S4 in Supporting Information). The hysteresis seen in Figure 2 is commonly observed when both semicrystalline and amorphous diblock copolymers are heated and cooled across the order−disorder transition.[25,26]

The data in Figure 2 indicate that the PEO−PSLiTFSI(5.0−3.2) diblock copolymer exhibits a reversible order-to-disorder transition (ODT) between 50 and 55 °C. The ODT in block copolymers with or without salt had been studied extensively.[12,27,28] In all cases, the transition is accompanied by an abrupt increase in the width of the primary SAXS peak. The broad peak obtained from the disordered phase is a signature of large amplitude concentration fluctuations. In contrast, the primary peak is absent in disordered PEO−PSLiTFSI(5.0−3.2) indicating the remarkable absence of concentration fluctuations. Note that the higher-order scattering peaks are detected at 50 °C, while neither primary nor higher-order peaks are evident at 55 °C.

Differential scanning calorimetry (DSC) experiments on PEO−PSLiTFSI copolymers indicate the presence of a melting peak at 55 °C. The DSC data are shown in the Supporting Information, Figure S2. The observed melting peaks in PEO−PSLiTFSI are qualitatively similar to those seen in the PEO homopolymer. This observation, in combination with data presented in Figure 2, suggests that microphase separation in PEO−PSLiTFSI is driven by the crystallization of the PEO block.

The lamellar morphology of PEO−PSLiTFSI(5.0−3.2) at room temperature was confirmed by dark field scanning transmission electron microscopy (STEM) as shown in Figure 3. The d spacing determined by STEM is 23 nm which is in

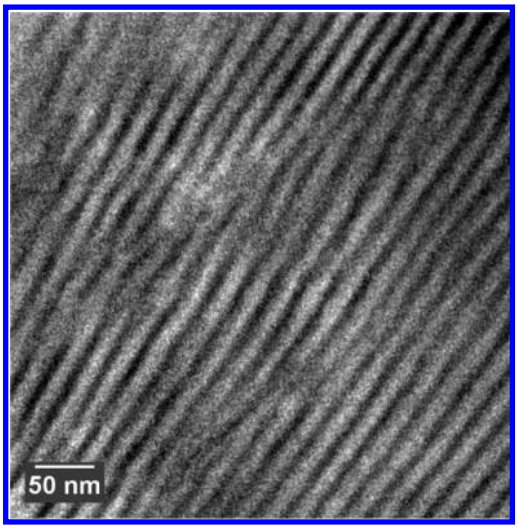

Figure 3. Dark field scanning transmission electron micrograph of PEO−PSLiTFSI(5.0−3.2), r = 0.088. The bright phase represents PEO-rich lamellae.

reasonable agreement with SAXS measurements. It is evident that PEO crystallization is confined within the microphase-separated structure.[29]

The temperature dependence of the conductivity of PEO−PSLiTFSI(5.0−3.2) is shown in Figure 4. At room temperature, the conductivity is 3.0×10^{-8} S cm^{-1}. The conductivity increases from 7.4×10^{-8} S cm^{-1} at 45 °C to 2.7×10^{-5} S cm^{-1} at 60 °C. A further increase in temperature results in a slower increase in conductivity, reaching a value of 3.8×10^{-4} S cm^{-1} at 90 °C. Also shown in Figure 4 is the temperature

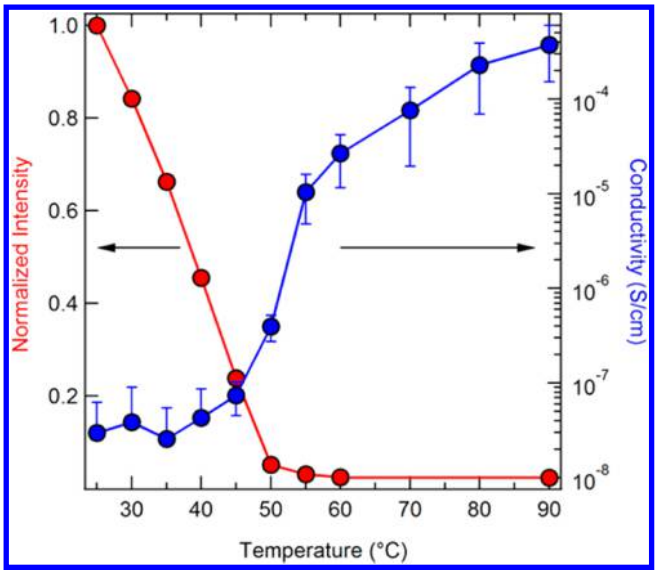

Figure 4. Conductivity and SAXS results of the PEO−PSLiTFSI electrolyte. The temperature dependence of the ionic conductivity (blue circles) and normalized SAXS intensity at q = 0.228 nm^{-1} (red circles) for PEO−PSLiTFSI(5.0−3.2), r = 0.088. Intensity at each temperature was normalized by the measured value at 25 °C.

dependence of the SAXS intensity at q = 0.228 nm^{-1} in the vicinity of the primary peak. There is a correlation between morphology and conductivity: high conductivity values are obtained when the sample is disordered and the normalized $I(q$ = 0.228 nm$^{-1})$ is nearly zero. This suggests that the migration of the lithium ions into a PEO-rich environment coincides with homogenization of the block copolymer microstructure. Further work is needed to establish the quantitative relationship between SAXS profiles and conductivity. To verify the morphology−conductivity relationship described above, we performed in situ SAXS experiments wherein the conductivity was measured concurrently with the SAXS experiment during a heating run. The conductivity data obtained during this run are included along with three separate ex situ conductivity measurements to obtain the values and error bars shown in Figure 4. The SAXS experiments were also repeated several times.

The PEO−PSLiTFSI(5.0−3.2) electrolyte was placed between two lithium foils, and the current needed to sustain a potential drop of 80 mV (ΔV) across the electrodes was measured as a function of time at 90 °C.[30−32] The results of this experiment are shown in Figure 5. The current density values obtained when the experiment was started and after 1 h were $I^0 = 6.99 \times 10^{-2}$ and $I^\infty = 6.90 \times 10^{-2}$ mA cm^{-2}, respectively. The results of ac impedance measurements before starting the experiment and after its completion are shown in the inset in Figure 5. The Nyquist plot of the impedance data contains two semicircles, a small semicircle representing electrolyte resistance, R_{elect}, and a large semicircle representing interfacial resistances, R_{int}.[33] The resistance values obtained before and after the cell polarization are $R_{elect}{}^0 = 127\ \Omega$ cm^2, $R_{elect}{}^\infty = 119\ \Omega$ cm^2, $R_{int}{}^0 = 1018\ \Omega$ cm^2, and $R_{int}{}^\infty = 1028\ \Omega$ cm^2, respectively.

The ionic conductivity values obtained from symmetrical cells using either lithium or aluminum electrodes are similar. In principle, determination of cation transference number, t^+, requires knowledge of salt activity coefficients.[28] In typical lithium battery electrolytes, the ratio I^∞/I^0 obtained during the

dx.doi.org/10.1021/mz5001948 | ACS Macro Lett. 2014, 3, 510−514

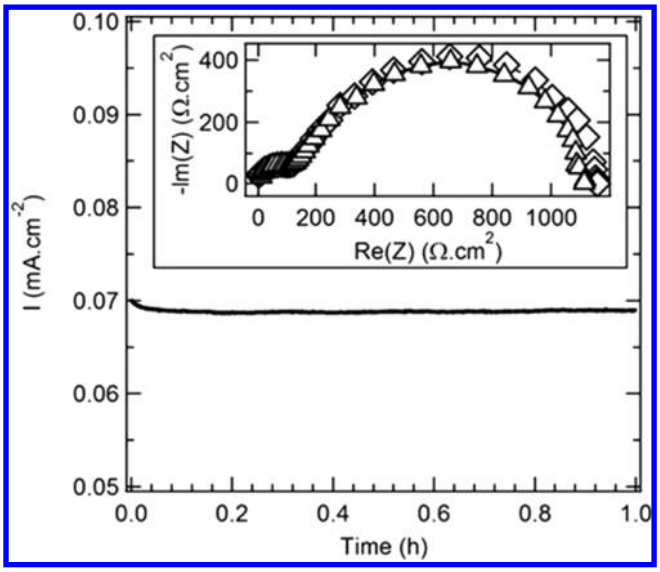

Figure 5. Transference number determination of the PEO−PSLiTFSI electrolyte. Current density as a function of time for PEO−PSLiTFSI(5.0−3.2) during an 80 mV polarization experiment at 90 °C. The inset shows the ac impedance of the cell (◊) before and (Δ) after polarization.

polarization experiment described in the preceding paragraph is about 0.3. In contrast, the value of I^{∞}/I^{0} obtained from PEO−PSLiTFSI(5.0−3.2) is 0.99. This implies that most of the current in our electrolyte is carried by the cation. In this case, the cation transference number, t^{+}, is approximately given by eq 1.

$$t^{+} = \frac{I^{\infty}(\Delta V - I^{0}R_{\mathrm{int}}^{0})}{I^{0}(\Delta V - I^{\infty}R_{\mathrm{int}}^{\infty})} \quad (1)$$

This gives $t^{+} = 0.95$. To a very good approximation, our PEO−PSLiTFSI(5.0−3.2) electrolyte is a single-ion-conductor.

The DSC, conductivity, and transference number results presented here are qualitatively consistent with those reported in ref 9. To assess the generality of our conclusions, we also studied the morphology−conductivity relationship in PEO−PSLiTFSI(5.0−2.0) diblock copolymer with $r = 0.056$. The data obtained from this sample are very similar to those obtained from PEO−PSLiTFSI(5.0−3.2) and thus presented in the Supporting Information, Figure S3.

The morphology−conductivity relationship derived from the results is pictured in Figure 6. At low temperatures, below 50 °C, we have an ordered microphase-separated structure with crystalline PEO-rich domains and glassy PSLiTFSI-rich domains ($T_{g,\ \mathrm{PSLiTFSI}} = 160$ °C). The Li^{+} and $TFSI^{-}$ ions form clusters in the glassy domains. The concentration of lithium ions in the PEO-rich domains is negligible, and this results in very low conductivity values (below 10^{-7} S cm^{-1}). At high temperatures, above 50 °C, we have a disordered morphology wherein amorphous PEO and PSLiTFSI blocks are intimately mixed, and most of the ions are no longer in clusters. A majority of the lithium ions in this state are "mobile", and conductivity values as high as 3.8×10^{-4} S cm^{-1} are obtained at 90 °C.

In conclusion, we have shown that the transfer of lithium ions from the glassy PSLiTFSI-rich domains into a PEO-rich environment results in disordered and highly conductive single-ion-conducting block copolymer electrolytes. The ability to design electrolytes wherein most of the current is carried by the lithium ions, to sequester them in nonconducting domains, and release them when necessary has the potential to enable new strategies for controlling the charge−discharge characteristics of rechargeable lithium batteries.

■ ASSOCIATED CONTENT

Supporting Information

Additional experimental details, SAXS, and conductivity results of PEO−PSLiTFSI(5.0−2.0) single-ion-conducting block copolymer electrolyte. This material is available free of charge via the Internet at http://pubs.acs.org.

■ AUTHOR INFORMATION

Corresponding Author

*E-mail: nbalsara@berkeley.edu.

Notes

The authors declare no competing financial interest.

■ ACKNOWLEDGMENTS

This work was primarily supported as part of the Joint Center for Energy Storage Research, an Energy Innovation Hub funded by the U.S. Department of Energy (DOE), Office of

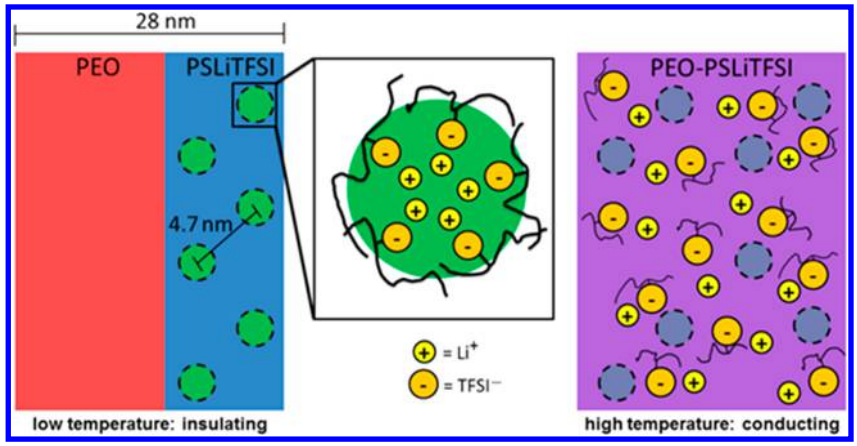

Figure 6. Schematics of the single-ion conducting block copolymer electrolyte at low and high temperatures. At low temperatures, the PEO (red) and PSLiTFSI (blue) blocks are microphase separated, and the ions are clustered (green circles). At high temperatures, the PEO and PSLiTFSI blocks are mixed (purple); the clusters (gray circles) are nearly dissolved; and the lithium ions are mobile.

Science, Basic Energy Sciences (BES). X-ray scattering research at the Advanced Light Source was supported by DOE, Office of Science, BES. The electrochemical testing equipment was supported by the Assistant Secretary for Energy Efficiency and Renewable Energy, Office of Vehicle Technologies of the U.S. Department of Energy under Contract DE-AC02-05CH11231 under the Batteries for Advanced Transportation Technologies (BATT) Program. Work at the Molecular Foundry, Lawrence Berkeley National Laboratory was supported by DOE, Office of Science, BES under Contract No. DE-AC02-11231. STEM work was provided by the Electron Microscopy of Soft Matter Program from the Office of Science, Office of Basic Energy Sciences, Materials Sciences and Engineering Division of the U.S. Department of Energy under Contract No. DE-AC02-05CH11231. The STEM experiments were performed as user projects at the National Center for Electron Microscopy, Lawrence Berkeley National Laboratory, under the same contract. We thank Dr. Eric Schaible for his help at Advanced Light Source, Lawrence Berkeley National Laboratory. We also gratefully acknowledge Jacob L. Thelen for helpful discussions.

REFERENCES

(1) Newman, J.; Thomas-Alyea, K. E. *Electrochemical Systems*, 3rd ed.; John Wiley & Sons, Inc.: Hoboken, NJ, 2004.
(2) Doyle, M.; Fuller, T. F.; Newman, J. *Electrochim. Acta* **1994**, *39* (13), 2073−2081.
(3) Hallinan, D. T.; Balsara, N. P. *Annu. Rev. Mater. Res.* **2013**, *43*, 503−525.
(4) Hsu, W. Y.; Gierke, T. D. *J. Membr. Sci.* **1983**, *13* (3), 307−326.
(5) Beers, K. M.; Balsara, N. P. *ACS Macro Lett.* **2012**, *1*, 1155−1160.
(6) Sun, X.-G.; Hou, J.; Kerr, J. B. *Electrochim. Acta* **2005**, *50*, 1139−1147.
(7) Dou, S.; Zhang, S.; Klein, R. J.; Runt, J.; Colby, R. H. *Chem. Mater.* **2006**, *18*, 4288−4295.
(8) Ryu, S.-W.; Trapa, P. E.; Olugebefola, S. C.; Gonzalez-Leon, J. A.; Sadoway, D. R.; Mayes, A. M. *J. Electrochem. Soc.* **2005**, *152* (1), A158−A153.
(9) Bouchet, R.; Maria, S.; Meziane, R.; Aboulaich, A.; Lienafa, L.; Bonnet, J.-P.; Phan, T. N. T.; Bertin, D.; Gigmes, D.; Devaux, D.; Denoyel, R.; Armand, M. *Nat. Mater.* **2013**, *12*, 452−457.
(10) Eitouni, H. B.; Balsara, N. P. In *Physical Properties of Polymers Handbook*, 2nd ed.; Mark, J. E., Ed.; Springer: New York, 2007; Chapter 19, pp 339−356.
(11) Young, W. S.; Epps, T. H. *Macromolecules* **2009**, *42*, 2672−2678.
(12) Teran, A. A.; Balsara, N. P. *J. Phys. Chem. B* **2014**, *118*, 4−17.
(13) Panday, A.; Mullin, S. A.; Gomez, E. D.; Wanakule, N.; Chen, V. L.; Hexemer, A.; Pople, J.; Balsara, N. P. *Macromolecules* **2009**, *42*, 4632−4637.
(14) Ghosh, A.; Wang, C.; Kofinas, P. *J. Electrochem. Soc.* **2010**, *157* (7), A846−A849.
(15) Capuano, F.; Croce, F.; Scrosati, B. *J. Electrochem. Soc.* **1991**, *138* (7), 1918−1922.
(16) Appetecchi, G. B.; Zane, D.; Scrosati, B. *J. Electrochem. Soc.* **2004**, *151* (9), A1369−A1374.
(17) Evans, J.; Vincent, C. A.; Bruce, P. G. *Polymer* **1987**, *28* (13), 2324−2328.
(18) Watanabe, M.; Nishimoto, A. *Solid State Ionics* **1995**, *79*, 306−312.
(19) Bouchet, R.; Aboulaich, A.; Maria, S.; Phan, T.; Gigmes, D.; Bertin, D.; Meziane, R.; Bonnet, J.-P.; Armand, M. Int. Patent WO2013/034848 A1, 2013.
(20) Eitouni, H. B.; Balsara, N. P. *J. Am. Chem. Soc.* **2004**, *126*, 7446−7447.
(21) Yuan, R.; Teran, A. A.; Gurevitch, I.; Mullin, S. A.; Wanakule, N. S.; Balsara, N. P. *Macromolecules* **2013**, *46*, 914−921.
(22) Yarusso, D. J.; Cooper, S. L. *Macromolecules* **1983**, *16*, 1871−1880.
(23) Wang, W.; Tudryn, G. J.; Colby, R. H.; Winey, K. I. *J. Am. Chem. Soc.* **2011**, *133*, 10826−10831.
(24) Kim, S. Y.; Park, M. J.; Balsara, N. P.; Jackson, A. *Macromolecules* **2010**, *43*, 8128−8135.
(25) Rangarajan, P.; Register, R. A.; Fetters, L. J.; Bras, W.; Naylor, S.; Ryan, A. J. *Macromolecules* **1995**, *28*, 4932−4938.
(26) Lee, S.; Gillard, T. M.; Bates, F. S. *AIChE J.* **2013**, *59* (9), 3502−3513.
(27) Leibler, L. *Macromolecules* **1980**, *13* (6), 1602−1617.
(28) Khandpur, A. K.; Forster, S.; Bates, F. S.; Hamley, I. W.; Ryan, A. J.; Bras, W.; Almdal, K.; Mortensen, K. *Macromolecules* **1995**, *28* (26), 8796−8806.
(29) Loo, Y.-L.; Register, R. A.; Ryan, A. J. *Macromolecules* **2002**, *35*, 2365−2374.
(30) Blonsky, R. M.; Shriver, D. F.; Austin, R.; Allcock, H. R. *Solid State Ionics* **1986**, *18/19*, 258−264.
(31) Bruce, P. G.; Vincent, C. A. *J. Electroanal. Chem.* **1987**, *225*, 1−17.
(32) Doyle, M.; Newman, J. *J. Electrochem. Soc.* **1995**, *142* (10), 3465−3468.
(33) Bouchet, R.; Lascaud, S.; Rosso, M. *J. Electrochem. Soc.* **2003**, *150* (10), A1385−A1389.